Solid State Ionics 1 (1980) 411–423

THE ELECTRICAL CONDUCTIVITY OF δ-Bi_2O_3 STABILIZED BY ISOVALENT RARE-EARTH OXIDES R_2O_3

H.T. CAHEN, T.G.M. VAN DEN BELT, J.H.W. DE WIT and G.H.J. BROERS
Department of Inorganic Chemistry, State University Utrecht, 3522 AD Utrecht, The Netherlands

Received 1 April 1980; in final form 16 July 1980

The phenomenon of δ-phase stabilization in the systems $(Bi_2O_3)_{0.75}(R_2O_3)_{0.25}$ where R = lanthanide metal (including La, but Pm excepted) was investigated. The electrical conductivity of those systems, which did show δ-stabilization, was investigated; the system $(Bi_2O_3)_{1-x}(Yb_2O_3)_x$ was studied in more detail. A Vegard-like relation between the cubic cell-axis and cationic radius of the substituted trivalent metal ion was found. A model is presented which accounts for results of electrical conductivity measurements and thermogalvanic measurements as well.

1. Introduction

Solid Bi_2O_3 was found to be an ionically conducting material ($t_{O^{2-}} = 1.0$) in the temperature range 730–824°C (mp) [1]. The specific electrical conductivity σ of this δ phase is ≈1 Ω^{-1} cm^{-1} [1–4]; its structure is (defect) fluorite with two vacant oxygen ion sites per unit cell [5–8]. In heating direction, from room temperature up to the α → δ transition at 730°C, conduction is (mainly) electronic [1]; the σ value of this α-phase is about three decades lower than σ of the δ phase [1–4]. The structure of the low-temperature phase is monoclinic [5,7–10]. In cooling direction, starting from a temperature above 730°C, the δ phase may (metastably) persist down to 639°C [2–4, 11, 12] and the sudden, strongly exothermic transition to the α phase is accompanied with a volume decrease of 7% [11,13]. Besides, two other metastable phases may come into existence: the tetragonal β phase [5,7,8,14,15] somewhere between 650 and 330°C [2,4,11,12] and the bcc γ phase [5,7,8,11] somewhere between 639 and 500°C [4,11,12].

δ-Bi_2O_3 would be an interesting material for practical purposes, e.g. as a solid electrolyte in galvanic cells or in an oxygen sensor, if it could be obtained at lower temperatures without too much loss of its exceptionally high (O^{2-}) ionic conductivity. Furthermore, partial replacement of Bi^{3+} ions in the cationic δ sublattice by less noble (preferably isovalent) cations could enhance the thermodynamic stability against reducing conditions. A variety of oxides have been claimed to be able to stabilize δ-Bi_2O_3 towards room temperature [6,14,16–32]; as for stabilization by rare-

Table 1
Survey of R_x systems which did (right part) or did not (left part) show δ-stabilization. An asterisk denotes this work. R_x stands for the rare-earth/bismuth mixed oxide with x = mole fraction of RE oxide

R	Atomic number	No δ-stabilization found in ref.	δ-stabilization observed in ref.
La	57	[6,11,23]*	[6]
Ce	58	[6,23]*	[22]
Pr	59	[23]*	[14]
Nd	60	[23]*	[6,14]
Pm	61		
Sm	62	[11,23]*	
Eu	63	[23]*	
Gd	64	*	[23,26]
Tb	65		[23]*
Dy	66		[23,43]*
Ho	67		[23]*
Er	68		[23,30]*
Tm	69		*
Yb	70	[23]	*
Lu	71	[11,23]	*

earth oxides information is gathered in table 1. As may be seen from table 1 there is some confusion about the δ-stabilizing capability of the rate-earth oxides; therefore it seemed interesting to investigate once again whether the lanthanide oxides can stabilize δ-Bi_2O_3 towards room temperature. Furthermore, since hardly any data are available concerning electrical conductivity, it was measured for those systems, which did show δ-structure stabilization. Finally, a model is presented which accounts both for results of electrical conductivity measurements and thermogalvanic measurements [34–36].

2. Experimental and results

In order to check whether the oxides of the lanthanides, including La (but with the exception of Pm, not being available), are able to stabilize the δ structure of Bi_2O_3, specimens of about 25 mole% R_2O_3 in Bi_2O_3 were prepared as follows: After weighing appropriate amounts of analytical grade Bi_2O_3 (Baker) and R_2O_3 (Merck, Fluka, BDH) in a polyethylene vessel the mixture was slurried in acetone in the same vessel for ≈ 1 h after which the acetone was decanted and further blown off by an airstream. The dried mixture was transferred into a platinum crucible, sintered in air at 780°C for ≈ 17 h and then cooled to ambient in ≈6 h. The specimen then was grounded in an agate mortar.

From Debye–Scherrer exposures (Cu Kα radiation, λ = 1.5418 Å) we found that

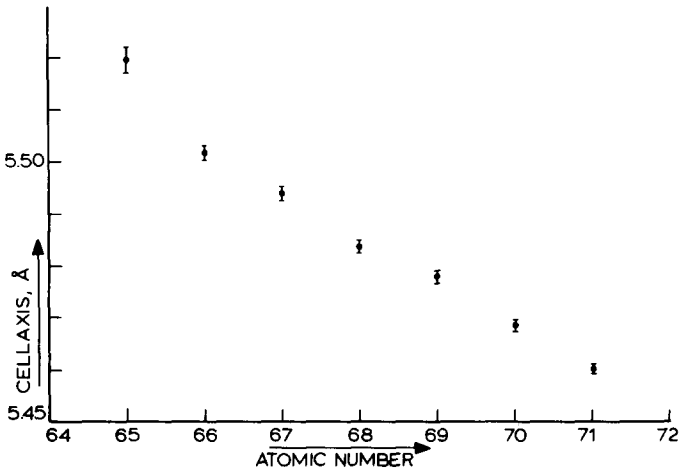

Fig. 1. Cubic cell axis versus atomic number of R for $R_{0.25}$.

the oxides of atomic number 65 = Tb through to 71 = Lu stabilized the fcc structure of δ-Bi_2O_3 at room temperature, whereas all other oxides (57 = La–64 = Gd) did not. All δ-stabilized oxides were orange-coloured at room temperature; the others all were yellow-coloured.

In order to exclude the influence of slight variations in composition, samples of 25.00 ± 0.01 mole% R_2O_3 in Bi_2O_3 (R = Tb(65)–Lu(71)) were prepared the same way as described above. Diffraction exposures now were obtained with the aid of a Guinier–Johannson camera (Cu $K\alpha_1$, radiation, λ = 1.5401 Å) using Si as internal standard. Cell-axis calculation was performed by aid of a powder pattern computer program described by Langford [37,38]. In fig. 1 these cell axes are plotted versus atomic number, their numerical values are given in table 2. For electrical conductivity measurements pellets of ≈ 0.8 cm diameter and ≈ 0.5 cm thickness were pressed in a stainless steel holder at ≈1000 kgf cm^{-2}. Before pressing, some stearic acid slurried in acetone was added to the powder in order to avoid sticking problems. Pellets were placed on a platinum sheet and sintered in air at 780°C for ≈60 h and subsequently cooled to room temperature in ≈6 h. Then they were platinum painted (Dégussit Pt-L 42) and heated in air at 400°C for ≈15 min.

Electrical conductivity measurements were performed on the pellets in an appropriate quartz cell. A pellet was placed between two platinum sheets ‡ at a distance of ≈2 mm from a Pt/Pt, 10% Rh thermocouple. Electrical conductivity was measured using a Wayne–Kerr B 642 bridge at f = 1592 Hz ($\omega = 10^4$ rad s^{-1}). No significant frequency dispersion was observed from 1000 Hz to 100 kHz. For more de-

‡ In contradiction to the pure δ-Bi_2O_3 [3,30], no severe contamination of these mixed oxides was observed.

Table 2
Cubic cell axis in the $R_{0.25}$ system for R = Y, Gd–Lu

R	Atomic number	$r_{R^{3+}}$ ref. [39]	Cubic cell axis (Å)			
			ref. [23]	refs. [25,26]	refs. [30,34]	this work
Gd	64	1.06	5.524			
Tb	65	1.04	5.504			5.519
Dy	66	1.03	5.487		5.496	5.502
Ho	67	1.02	5.485			5.494
Y	39	1.015	5.520	5.51		5.493
Er	68	1.00	5.475		5.474	5.484
Tm	69	0.99				5.478
Yb	70	0.98				5.469
Lu	71	0.97				5.461

tailed information we refer to ref. [40]. Electrical conductivity $> 0.1\ \Omega^{-1}$ was measured using a four-probe method. Temperature was raised (or lowered) at 3°C min^{-1} We found that results from conductivity measurements using this rate did not deviate more than 10% (within one decade of conductivity) from equilibrium measurements (i.e. the final, constant value conductivity at a set temperature). The results of electrical conductivity measurements, performed in heating direction on the $R_{0.25}$ systems ‡ (R = Tb–Lu) are given in fig. 2. The influence of x upon the conductivity was measured on the Yb_x system with $x = 0.10, 0.20, 0.25, 0.30$ and 0.35. These results are given in fig. 3. The possible occurrence of solid state transformations or (partial) melting was checked by some differential thermal analyses (DTA). Measurements were performed on $R_{0.25}$, with R = Tb, Dy and Ho, and on Yb_x with $x = 0.1, 0.2$ and 0.3. Measurements between room temperature and 950°C were performed in air using a platinum cucible (sample amounting ≈ 2.5 g).

Only the $Yb_{0.1}$ system showed an isothermal effect (in heating direction) at ≈640°C; in all other systems no thermal arrests were detectable. Furthermore, with the aid of a Guinier–Lenné camera (Cu Kα radiation) a high-temperature exposure was made on the $Yb_{0.25}$ system in heating direction at a rate of 13°C h^{-1}. The exposure revealed co-appearance of other lines at ≈700°C.

The samples were characterized also through electron microscopy. They were shown to be not very disperse, with a typical specific surface area of 0.25 m^2/g for e.g. $Y_{0.25}$. More details are given in ref. [40].

‡ For brevity reasons "binary" systems $(Bi_2O_3)_{1-x}(R_2O_3)_x$ will be denoted by R_x.

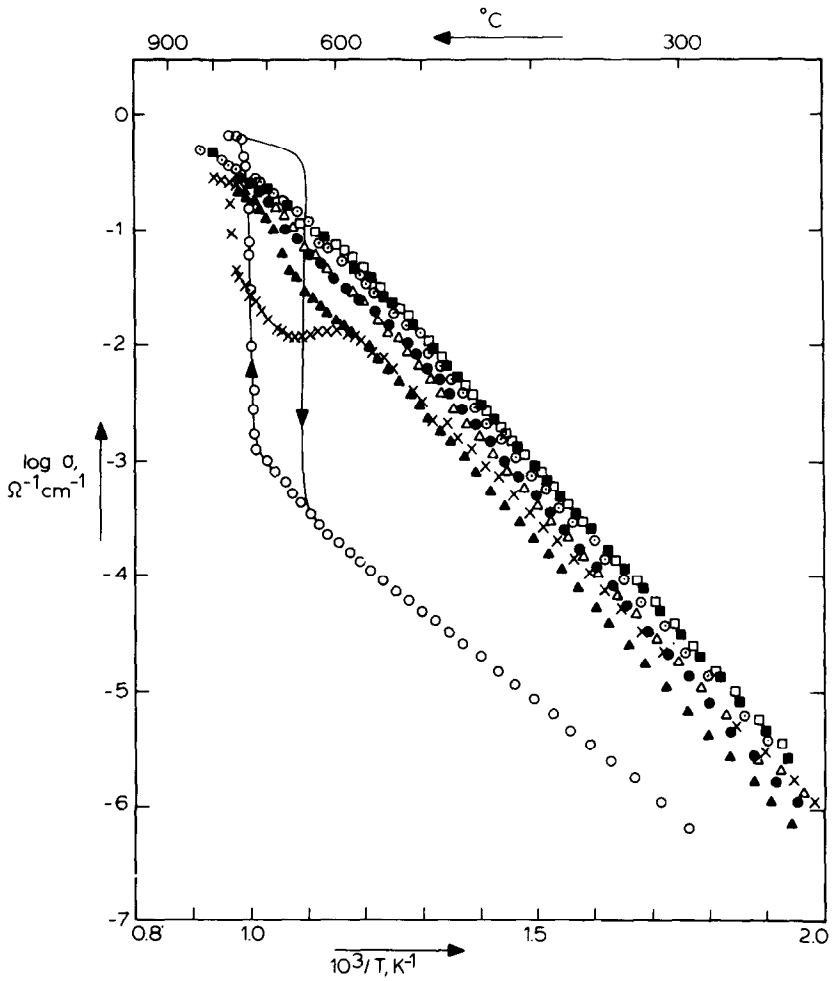

Fig. 2. Electrical conductivity σ of $R_{0.25}$, measured in air in heating direction; for comparison σ of pure Bi_2O_3 is given as well (○). ×: R = Tb(65); ■: R = Dy(66); □: R = Ho(67); ⊙: R = Er(68); △: R = Tm(69); ●: R = Yb(70); ▲: R = Lu(71).

3. Discussion

3.1. Structural considerations

From all $R_{0.25}$ systems under investigation only those systems with R = Tb–Lu, i.e. atomic numbers 65–71, proved to stabilize the fcc structure down to room temperature. As for the systems with R = Tb(65)–Er(68) this δ stabilization was also

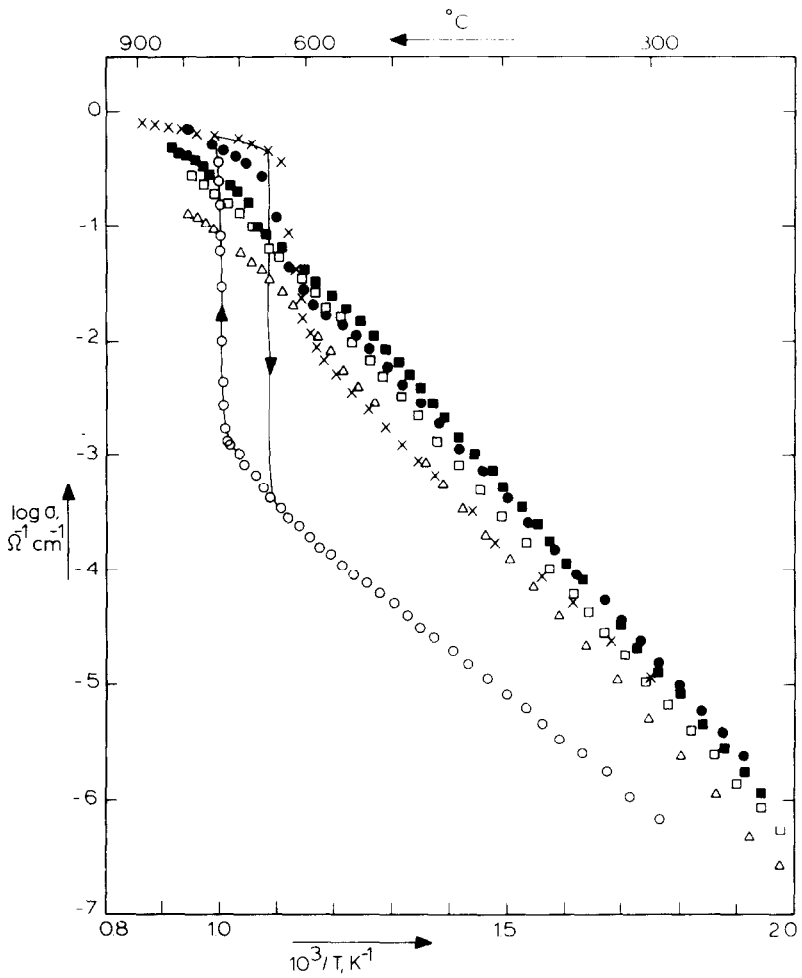

Fig. 3. Electrical conductivity σ of Yb_x, measured in air in heating direction; for comparison σ of pure Bi_2O_3 is given as well (○). ×: $x = 0.10$, ●: $x = 0.20$; ■: $x = 0.25$; □: $x = 0.30$; △: $x = 0.35$.

reported by Datta and Meehan [23], however, for R = Yb(70) and Lu(71) he found a rhombohedral phase (he did not investigate the Tm(69) system). On the other hand, he found δ stability in the $Gd_{0.25}$ (64) system whereas we did not. Takahashi et al. [26] found a rhombohedral structure in the $Gd_{0.20}$ system when slowly cooled from sintering temperature (900°C) to room temperature; quenching the specimen to room temperature in a few minutes revealed the fcc form. Verkerk et al. [30] found that the $Er_{0.15}$ system exhibited the δ structure when cooled down from 800°C to room temperature by 0.5°C min^{-1} or when quenched from sintering tem-

perature to room temperature in a few minutes. However, when annealed at 625°C for ≈10 days and then cooled to room temperature within some hours he found the α (monoclinic), the β (tetragonal), and a rhombohedral structure as well. Our high-temperature exposure on the $Yb_{0.25}$ system revealed the appearance of other phase(s) at ≈700°C, whereas all Guinier–Johannson ambient exposures on the $R_{0.25}$ systems (with R = Tb–Lu) did not show but the fcc structure. Cooling rate from sintering temperature to room temperature seems to be a dominating factor with respect to the structure(s) finally obtained at room temperature. Although our samples were cooled rather slowly (within ≈6 h) they therefore do not necessarily represent an equilibrium situation. DTA is no appropriate tool to investigate these long-term effects. On the other hand, investigation with the aid of high-temperature X-ray diffraction may cause contamination by Pt and subsequent effects on crystal structure. Harwig and Gerards [3] found that pellets supplied with Pt-paint contained 0.04–0.06 wt% Pt after a series of electrical conductivity measurements. DTA tests in heating direction in air on the system Bi_2O_3–5 wt% Pt revealed a strong exothermic effect at ≈660°C. Verkerk et al. [30] found ≈ 2% Pt in a specimen after a high-temperature Guinier investigation up till ≈680°C. Table 2 shows that the unit cell axes of the $R_{0.25}$ systems are in good accord with those found by Datta and Meehan [23] and Verkerk et al. [30]. Fig. 1 reveals a fairly linear relationship between cell axes and atomic number of R, which if course is a reflection of the lanthanide ion contraction. Furthermore, Datta and Meehan [23], Takahashi et al. [26], and Verkerk et al. [30] found a linear decrease of the cell axes with increasing x in the R_x systems, with R = Gd, Gd, and Er, respectively. This behaviour was also found in the Y_x system by Datta and Meehan [23], and Takahashi et al. [25]. Apparently the cell axis in a M_x system is determined both by the radius of M^{3+} and the value of x. For $x = 0.25$ one may tentatively calculate the lower critical radius limit of M^{3+}, assuming a fcc unit cell (space group Fm3m) with all M^{3+} ions on corner sites, all Bi^{3+} ions on face centers and all O^{2-} ions randomly distributed on tetrahedral sites. Ionic radii, given by Shannon and Prewitt [39] were used. Based upon this model, the lower critical radius limit for δ stabilization in δ-$M_{0.25}$ system should fall at $r(M^{3+}) > 1$ Å, because smaller radii would yield interatomic O^{2-}–O^{2-} distances less than twice the O^{2-} radius (1.38 Å). Experiments with the $In_{0.25}$ system (radius In^{3+} = 0.92 Å proved that no δ stabilization could be obtained, in accordance with this simple, highly symmetrical hard-sphere model.

3.2. Phenomenological description of the conductivity data

Fig. 2 shows the measured conductivities σ at 1592 Hz of the $R_{0.25}$ systems for R = Tb(65) to Lu(71). Crudely taken, all log σ versus $1/T$ curves have an analogous course except for R = Tb(65), which shows distinct anomalies. In the high-temperature range (> 560°C) the conductivities approach that for pure δ-Bi_2O_3. However, the activation enthalpy has a somewhat higher value and the absolute conductivity is somewhat smaller. At lower temperatures the apparent activation enthalpy for

the $R_{0.25}$ series is far greater (1.15 eV) than would be expected from the extrapolated value for pure δ-Bi_2O_3 (≈ 0.3 eV [3]). From a high-resolution plot (not shown) a transition region (600–700°C) is seen to occur for the Lu(71), Yb(70), Tm(69), and Er(68) systems, in decreasing order of importance. For Ho(67) and Dy(66) there is no such an effect. Also there is a clear trend in the sequence of isothermal conductivities in the lower range 240–560°C; one obtains in terms of σ: Lu(71) < Yb(70) < Tm(69) < Er(68) < Ho(67) < Dy(66). Again the location of Tb(65) is anomalous (compare also fig. 1), which may point to an upper critical radius limit in the vicinity of Gd(64) and Tb(65). The location of non-R^{3+} ion $Y^{3+}_{0.25}$ between the curves of fig. 2 (not shown) is in good accordance with its intermediate radius valence between Ho^{3+}(67) and Er^{3+}(68) in table 2.

Fig. 3 shows the measured conductivities σ at 1592 Hz of the Yb_x system, with $x = 0.10, 0.20, 0.25, 0.30$ and 0.35. In the high-temperature range (> 560°C) the conductivities approach that for pure δ-Bi_2O_3. However, with increasing content of Yb_2O_3 the activation enthalpy has a somewhat higher value and the absolute conductivity is somewhat smaller. One obtains in terms of σ as a function of x: 0.10 > 0.20 > 0.25 > 0.30 > 0.35. At lower temperatures (240–560°C) the apparent activation enthalpy for the Yb_x series is far greater (1.15 eV) than would be expected from the extrapolated value (≈ 0.3 eV [3]) for pure δ-Bi_2O_3. Here an optimum value of σ is obtained at $x \approx 0.25$. The sequence of σ as a function of x is: 0.25 ≈ 0.20 > 0.30 > 0.35 ≈ 0.10. The same trend was also observed for the Y_x system.

3.3. Interpretation of the conductivity data

3.3.1. Introduction to theory

It can be taken for granted that the observed conductivities are due to mobile O^{2-} ions. Evidence from thermogalvanic measurements has been presented elsewhere [34,36]. These thermogalvanic data also showed discrepancy between the activation enthalpy for conduction (E_{ac}) and the heat of transport Q^* for pure δ-Bi_2O_3. Moreover, as compared with pure δ-Bi_2O_3, the heat of transport was found to be hardly influenced by the addition of RE oxides, in contrast with the value of E_{ac}. For these mixed oxides the heat of transport was nearly temperature independent over the accessible temperature range from ≈ 525 to 800°C and almost equal to the value for pure δ-Bi_2O_3 (0.18 versus 0.19 eV, respectively) in contrast with the value for E_{ac} (1.15 versus 0.30 eV, respectively). This seems rather surprising, e.g. the free ion model of Rice and Roth [41] predicts an equality of the two parameters. The free ion theory postulates the existence of an energy gap ϵ_0 in the ion density of states. Conduction occurs via the excitation of ions from localized states at zero energy into a continuum state above the gap, similar to the intrinsic activation process of a semiconductor. In this continuum state the ions contribute via the same "mobility" mechanism to both Q^* and E_{ac}, resulting in an equality of these two parameters. The energy gap ϵ_0 is to be considered as a static barrier resulting from

the static potential acting on the mobile ions due to the background lattice. Because this does not explain our results it seems logical to abandon the concept of the static barrier and to introduce a dynamical barrier. This leads us to the "lattice gas" model of Pardee and Mahan [42]. The dynamical processes are represented by the interaction of the mobile anions among themselves (the lattice gas) *and* the interaction of the anions with the cations (phonons). The ionic motion is allowed through a phenomenological hopping term. This term represents the average rate of hopping due to the thermal fluctuations of the dynamical processes. This theory, at least for low temperatures predicts $Q^* < E_{ac}$, in contradiction with the occasionally observed equality of these two parameters for fast ionic conductors. However, at high temperatures (as in our case) this theory could not describe the dynamics of fast ion conductors because the heat of transport was found to be independent of the main parameters: the dynamical ionic polaron energy E_b.

The proposed model is based on the extended lattice theory of Girvin [43]. In the tight bonding approach to band theory, which results in the concept of the electronic polaron, the narrow bands are assumed to originate from localized electronic states in potential wells. The same approach is now adopted for the ionic polaron. The main difference between the electronic and the ionic polaron results from the extreme difference in mass. Here the magnitude of the excitation energy of an ion in a potential well is of the same order as the phonon energy value, so that we should take into consideration all the excited levels and not only the ground state as was allowed in the case of electrons. Furthermore, the overlap between the low-energy states at neighbouring sites may be neglected (no tunneling). This results in a hopping term which is purely phenomenological in nature, as was already mentioned in section 1. It represents the average rate of hopping due to all thermal fluctuations. Now, the activation energy for conduction E_{ac}, being the experimentally accessible parameter concerning the hopping rate, is assumed to consist of a static and a dynamic term. The potential well of depth W at a lattice site (see fig. 4) consists of several vibrational states. Hopping from one well into another one can only

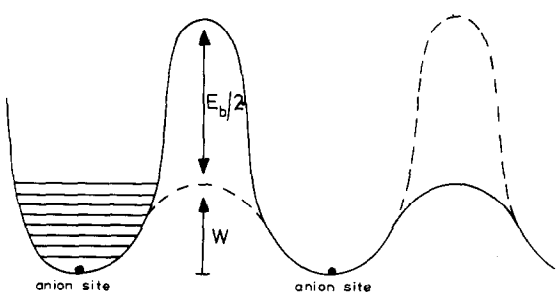

Fig. 4. Schematic illustration of the proposed model based on the extended lattice gas model of Girvin [39]. W represents the static barrier consisting of several vibrational states. $E_b/2$ represents the dynamical barrier.

occur after excitation to a high vibrational state, because the lower states are strongly localized. This is equivalent to the static part of the barrier of activation. This high vibrational state can couple with the phonons in the background lattice (polaron coupling). Both anion–anion coupling (for anionic conductors the lattice gas) and anion–cation coupling (the phonons) play a role. For high-temperature disordered phases the anion–cation polaron coupling is dominant [43]. This long-range polaron coupling is the dynamical part of the activation barrier (see fig. 4) and equal to the polaron binding energy $E_b/2$.

In this model it is assumed that for high-temperature disordered phases the static and dynamical barriers simply add up in their influence on the activation energy for conduction E_{ac} resulting in:

$$E_{ac} = W_{st} + (E_b/2)_{dyn} .$$

At sufficiently high temperatures the dynamic barrier does not contribute to the heat of transport Q^*, so that $Q^* = W_{st}$. Thus the implicit results of the lattice gas approach is as follows: At high temperatures the lattice gas disorders and the conductivity (E_{ac}) becomes dominated by the long-range polaron coupling ($E_b/2$) as we saw above, but the thermopower and thus the heat of transport Q^* (= W_{st}) saturates at a fixed value and is no longer correlated with the activation energy for conduction E_{ac}. Each "thermally" hopping particle carries a well defined amount of energy when it hops: $Q^* = W_{st}$. When the lattice is strongly disordered one can also expect that the heat of transport is very small, because Q^* represents the *excess* heat of a selected (non-average) ensemble of transported particles; where disorder is nearly complete hardly any selection will take place which is reflected in a very small value of Q^*. The static contribution $W = Q^*$ should be seen as a time averaged barrier, involving all mobile particles hopping from well to well at a comparatively slow rate (related to the heat diffusivity of the solid). The time constant of this process should be much larger than the one associated with the establishment of ionic conduction (10^{-11}–10^{-13} s).

3.3.2. Evaluation of the experimental results in connection with the proposed model

The most striking fact in the conductivity data is the low conductivity value for the mixed oxides below the α–δ transition temperature of pure Bi_2O_3 and the similarity of all the (high) activation enthalpies for the different RE additions, even for various concentrations. X-ray diffraction data proved the existence of a δ phase at room temperature in all cases. IR absorption spectroscopy performed on these mixed oxides at room temperature showed the disappearance of all typical absorption peaks of the original RE oxide and α-Bi_2O_3 which sustains our ideas on the existence of the (disordered) δ phase below the α–δ transition temperature of pure Bi_2O_3.

Therefore, at first sight it seems rather strange that the activation enthalpy for conduction has such a high value. One possible explanation would be the existence of a small amount of a second phase (with low conductivity) which could not be detected by X-ray diffraction because of its rather low resolution of ≈5%. The IR

absorption spectra were checked for their sensitivity to a second phase [44] with an even worse result of ≈20%. However, semi-micro DTA experiments, with a much better sensitivity did not prove the existence of a significant amount of second phase. Only in a few samples with a not-well defined temperature pretreatment were small inclusions of a second phase found, probably due to a non-equilibrium situation. We therefore reject the explanation based on a second phase. The observed behaviour confirms what should be expected if the extended lattice gas model is applied. The mere fact that X-ray analysis shows the existence of a structure with δ phase symmetry does not yet imply that the rigidity of the structure also remains the same as for the pure high-temperature δ phase. First, the lattice constant shrinks somewhat with the radius of the incorporated RE cation, which could influence the barrier height for the mobile oxygen anions. However, it seems not very likely that this small shrinkage (of the order of 1%) has such an enormous impact on the activation enthalpy for conduction. More important seems the fundamental difference between the electronic structure of the R^{3+} and the Bi^{3+} ions. The R^{3+} ions have a closed-shell structure: $[Xe]\,4f^n$, whereas the Bi^{3+} ion has a $6s^2$ lone pair: $[Xe]\,4f^{14}\,5d^{10}\,6s^2$ Bi^{3+} thus has a high polarizability which probably is the very reason that O^{2-} conduction in this solid substance may occur.

The high polarizability is the cause that in pure δ-Bi_2O_3 (≈ 650–729°C), where the lattice gas (O^{2-}–O^{2-} coupling) is disordered, the anion–cation coupling (O^{2-}–Bi^{3+}) (the phonons) only play a modest role resulting in a low value for the polaron binding energy E_b of the order of $2kT$. However, when the mixed oxides with the RE oxides are formed the coupling with the cations gets much stronger, resulting in a high value of the polaron binding energy E_b. The rigidity of the structure has little influence on the static part of the barrier formed by the background potential of the lattice which remains approximately constant. In fact, the static part of the barrier $W = Q^*$ remains constant over the whole temperature range as we found from the thermoelectric power ($Q^* = 0.19$ eV), thus sustaining our theory that *only* the increased anion–cation coupling determined the high value of E_{ac} and the resulting low conductivity at lower temperature. This theory can also explain the decreasing σ with decreasing (65 → 71) RE ion radius. The absolute differences between the isothermal conductivity values are rather small as compared with the large temperature dependency. This could very well result from the small shrinkage of the lattice which increases the anion–anion coupling (the lattice gas) only slightly. This implies that the heat of transport for doped samples should show slight differences for various dopants and concentrations inside the δ-stability range. In view of the uncertainty of the value of Q^* these differences are probably within experimental error.

Also the "transition region" around the α–δ phase transition temperature of pure Bi_2O_3 for Lu(71), Yb(70), Tm(69), and Er(68) in decreasing order of importance can be understood. For smaller cations the absolute value of σ also decreases under influence of the shrinkage of the lattice, which results in a stronger anion–anion coupling. This coupling then diminishes more explicitly for the smaller RE

cations at the "transition temperature". Above this temperature microparts of the lattice do really obtain the δ phase without experiencing the influence of the RE ions on the rigidity. The lattice does not really need the RE ions to obtain this struc ture at these temperatures. The resulting influence of these ions is seen in the still slightly steeper slope than for the pure material as a result of the somewhat increased anion–cation coupling (dynamical barrier). The concentration influence as seen in fig. 3 may simply indicate that within this range, $x = 0.10$–0.35, anion–cation coupling is hardly concentration sensitive (the slopes of the curves are nearly identical). The anion–anion coupling and the static barrier might be more sensitive to concentration effects resulting in different absolute conductivity values. The optimum value around $x = 0.25$ may result from correlation effects at high concentrations.

References

[1] T. Takahashi, H. Iwahara and Y. Hagai, J. Appl. Electrochem. 2 (1972) 97.
[2] C.N.R. Rao, G.V. Subba Rao and S. Ramdas, J. Phys. Chem. 73 (1969) 672.
[3] H.A. Harwig and A.G. Gerards, J. Solid State Chem. 26 (1978) 265.
[4] H.A. Harwig and A.G. Gerards, Thermochim. Acta 28 (1979) 121.
[5] L.G. Sillén, Arkiv Kemi 18 (1937) 1.
[6] G. Gattow and H. Schröder, Z. Anorg. Allg. Chem. 318 (1962) 176.
[7] H.A. Harwig, Z. Anorg. Allg. Chem. 444 (1978) 151.
[8] H.A. Harwig and J.W. Weenk, Z. Anorg. Allg. Chem. 444 (1978) 167.
[9] L.G. Sillén, Z. Krist. A103 (1941) 274.
[10] G. Malmros, Acta Chem. Scand. 24 (1970) 384.
[11] E.M. Levin and R.S. Roth, J. Res. Natl. Bur. Std. US 68A (1964) 189.
[12] R. Matsuzaki, H. Masumizu and Y. Seaki, Denki Kagaku 42 (1974) 578.
[13] C.A. Johnson, R.C. Brodt and J.H. Hoke, J. Am. Ceram. Soc. 58 (1975) 37.
[14] G. Gattow and D. Schütze, Z. Anorg. Allg. Chem. 328 (1964) 44.
[15] B. Aurovillius and G. Malmros, Kgl. Tekniska Högskolans Handlingar 291 (1972) 545.
[16] W.C. Schumband and E.S. Rittner, J. Am. Chem. Soc. 65 (1943) 1055.
[17] G. Gattow and D. Schütze, Naturwissenschaften 50 (1963) 546.
[18] G. Gattow, Z. Anorg. Allg. Chem. 298 (1959) 64.
[19] G. Gattow and H. Fricke, Z. Anorg. Allg. Chem. 324 (1963) 287.
[20] L.G. Sillén and B.A. Aurivillius, Z. Krist. 101 (1939) 483.
[21] E.M. Levin and R.S. Roth, J. Natl. Bur. Std. US 68A (1964) 197.
[22] F. Hund, Z. Anorg. Allg. Chem. 333 (1964) 248,
[23] R.K. Datta and J.P. Meehan, Z. Anorg. Allg. Chem. 383 (1971) 328.
[24] T. Takahashi and H. Iwahara, J. Appl. Electrochem. 3 (1973) 65.
[25] T. Takahashi, H. Iwahara and T. Arao, J. Appl. Electrochem. 5 (1975) 187.
[26] T. Takahashi, T. Esaka and H. Iwahara, J. Appl. Electrochem. 5 (1975) 197.
[27] T. Takahashi, T. Esaka and H. Iwahara, J. Appl. Electrochem. 7 (1977) 299.
[28] T. Takahashi, T. Esaka and H. Iwahara, J. Appl. Electrochem. 7 (1977) 303.
[29] T. Takahashi, H. Iwahara and T. Esaka, J. Electrochem. Soc. 10 (1977) 1563.
[30] M.J. Verkerk, K. Keizer and A.J. Burggraaf, J. Appl. Electrochem. 10 (1980) 81.
[31] T. Takahashi and H. Iwahara, Mat. Res. Bull. 13 (1978) 1447.
[32] T. Takahashi, H. Iwahara and T. Esaka, J. Electrochem. Soc. 124 (1977) 1563.

[33] M.J. Verkerk and A.J. Burggraaf, J. Electrochem. Soc., to be published.
[34] G.H.J. Broers, H.T. Cahen, A. Honders and J.H.W. de Wit, J. Appl. Electrochem. 10 (1980) 229.
[35] J.H.W. de Wit, T. Honders and G.H.J. Broers, Proceedings of Conference on Fast Ion Transport in Solids, Lake Geneva, Wisconsin, May 21–25, 1979.
[36] A. Honders and J.H.W. de Wit, J. Appl. Electrochem. 10 (1980) 409.
[37] J.I. Langford, J. Appl. Cryst. 4 (1971) 259.
[38] J.I. Langford, J. Appl. Cryst. 6 (1973) 190.
[39] R.D. Shannon and C.T. Prewitt, Acta Cryst. B25 (1969) 925.
[40] H.T. Cahen, Thesis, University of Utrecht (1980).
[41] M.J. Rice and W.L. Roth, J. Solid State Chem. 4 (1972) 294.
[42] W.J. Pardee and G.D. Mahan, J. Solid State Chem. 15 (1975) 310.
[43] S.M. Girvin, J. Solid State Chem. 25 (1978) 65.
[44] H.T. Cahen, J.H.W. de Wit, A. Honders, G.H.J. Broers and J.P.M. van den Dungen, Solid State Ionics 1 (1980) 425.